

RESEARCH

Open Access



Edible CaCO₃ nanoparticles stabilized Pickering emulsion as calcium-fortified formulation

Xiaoming Guo[†], Xiaoying Li[†], Leung Chan, Wei Huang and Tianfeng Chen^{*†}

Abstract

Background: Nanoparticles assembled from food-grade calcium carbonate have attracted attention because of their biocompatibility, digestibility, particle and surface features (such as size, surface area, and partial wettability), and stimuli-responsiveness offered by their acid-labile nature.

Results: Herein, a type of edible oil-in-water Pickering emulsion was structured by calcium carbonate nanoparticles (CaCO₃ NPs; mean particle size: 80 nm) and medium-chain triglyceride (MCT) for delivery of lipophilic drugs and simultaneous oral supplementation of calcium. The microstructure of the as-made CaCO₃ NPs stabilized Pickering emulsion can be controlled by varying the particle concentration (*c*) and oil volume fraction (*φ*). The emulsification stabilizing capability of the CaCO₃ NPs also favored the formation of high internal phase emulsion at a high *φ* of 0.7–0.8 with excellent emulsion stability at room temperature and at 4 °C, thus protecting the encapsulated lipophilic bioactive, vitamin D3 (VD3), against degradation. Interestingly, the structured CaCO₃ NP-based Pickering emulsion displayed acid-triggered demulsification because of the disintegration of the CaCO₃ NPs into Ca²⁺ in a simulated gastric environment, followed by efficient lipolysis of the lipid in simulated intestinal fluid. With the encapsulation and delivery of the emulsion, VD3 exhibited satisfying bioavailability after simulated gastrointestinal digestion.

Conclusions: Taken together, the rationally designed CaCO₃ NP emulsion system holds potential as a calcium-fortified formulation for food, pharmaceutical and biomedical applications.

Keywords: Pickering emulsion, CaCO₃, Gastrointestinal digestion, Bioresponsive

Background

Pickering emulsions, a type of emulsion stabilized by solid particles rather than molecular surfactants, have received growing attention in the food, cosmetic, and biomedical industries due to their stability, which ranges from months to years, high internal payload capacity and added functionality derived from the stabilizing particles themselves [1–4]. In the field of drug oral delivery

and release, Pickering emulsions enable the delivery of cargo to sites of interest (e.g., small intestine and colon) through passive diffusion-controlled or actuated release manners [1], relying on the combination of emulsifier properties and external triggers [5, 6]. When ingested, the stabilizing particles generally experience complex physicochemical changes as they are sequentially exposed to the human gastrointestinal (GI) tract, which encompasses the mouth, stomach, and small intestine [7–9]. GI-responsive fashion seems feasible if the particles can respond to these ‘internal’ stimuli from the GI environment. To achieve this goal, acid-sensitive Pickering emulsion system designs have been developed based

*Correspondence: tchentf@jnu.edu.cn

[†]Xiaoming Guo and Xiaoying Li contributed equally to this work
Department of Oncology, The First Affiliated Hospital, Department of Chemistry, Jinan University, Guangzhou 510632, China



© The Author(s) 2021. This article is licensed under a Creative Commons Attribution 4.0 International License, which permits use, sharing, adaptation, distribution and reproduction in any medium or format, as long as you give appropriate credit to the original author(s) and the source, provide a link to the Creative Commons licence, and indicate if changes were made. The images or other third party material in this article are included in the article's Creative Commons licence, unless indicated otherwise in a credit line to the material. If material is not included in the article's Creative Commons licence and your intended use is not permitted by statutory regulation or exceeds the permitted use, you will need to obtain permission directly from the copyright holder. To view a copy of this licence, visit <http://creativecommons.org/licenses/by/4.0/>. The Creative Commons Public Domain Dedication waiver (<http://creativecommons.org/publicdomain/zero/1.0/>) applies to the data made available in this article, unless otherwise stated in a credit line to the data.

on an environment that has many acid-labile particles. However, most of these particles were fabricated from synthetic materials that may raise safety concerns. Therefore, exploiting acid-sensitive Pickering emulsifiers that are non-toxic, biologically benign and compatible is of practical significance.

In the recent decade, there has been growing research interest in assembling particles using “generally regarded as safe” (GRAS) inorganic materials, such as hydroxyapatite, calcium phosphate, tri-calcium phosphate, and calcium carbonate, to maximize emulsion stabilization and minimize side effects [10–13]. Among the vast variety of materials, food-grade calcium carbonate (CaCO_3) has gained attention as a Pickering emulsifier, particularly in the food, pharmacy, and medical industries [14], as it is of substantial importance for three main reasons: (1) CaCO_3 is a recognized food additive and pharmaceutical ingredient that is advantageous for its low-cost and availability in large quantities [3]; (2) CaCO_3 particles can impart acid-responsive properties into the Pickering emulsion it stabilizes by virtue of its acid-soluble nature [15]; (3) functional properties (calcium fortification and acid neutralization capacity) can also be added to the Pickering emulsion after converting CaCO_3 particles into absorbable calcium ions once exposed to gastric acid [16]. Until now, CaCO_3 -based oil-in-water and water-in-oil Pickering emulsions have been reported [3, 17–19]. However, understanding the gastrointestinal fate of the CaCO_3 Pickering emulsion has been minimally investigated. In-depth understanding of how the particle characteristics, such as the density, size, and surface properties, affect its gastric digestion behavior is necessary given that oral ingestion is the preferred route for CaCO_3 Pickering emulsions.

Particle size control is crucial for the use of solid CaCO_3 as a Pickering emulsifier [2, 18, 20, 21]. Generally, the particle size should be at least one order of magnitude smaller than the targeted emulsion droplet size [2]. Nanosized CaCO_3 of different shapes (cube, sphere, and rod) has higher capabilities of forming a Pickering emulsion (mostly oil/water type) due to its finer size and partial wettability between both continuous and dispersed phases as compared to conventional CaCO_3 of micron-scale features [18, 22] as it allows CaCO_3 nanoparticles (NPs) to locate the droplet surface [20]. Another unique feature of CaCO_3 NPs is its large surface area, which offers hydrophobization availability to enhance the emulsification efficacy [3, 17, 23]. From the viewpoint of calcium-fortified food, CaCO_3 NPs would add value to the resulting Pickering emulsion as it favors a good calcium absorption rate, which has been supported by *in vivo* animal and clinic studies [24, 25].

In this study, we have reported a food-grade Pickering emulsion using CaCO_3 NPs as the stabilizer. First, we synthesized the CaCO_3 NPs (40–140 nm) through the *in situ* reaction of CO_2 and calcium hydroxide in an aqueous solution. Next, the CaCO_3 NPs were successfully used to prepare Pickering emulsions at oil volume fractions ranging from 0.2 to 0.8. Then, the CaCO_3 NP-based Pickering emulsion was used as a vehicle for delivering vitamin D3 (VD3) through the GI tract. VD3 was specially selected as a model compound, as it is of importance for two reasons: on the one hand, VD3 is well-soluble in oil and thereby is advantageous for the assessment of its bioavailability in the *in vitro* simulated GI analysis [26–28]; on the other hand, as VD3 is frequently formulated with CaCO_3 as a co-medication [29, 30], it could shed light on the conceptualization of the Pickering emulsion with enhanced calcium fortifying properties based on CaCO_3 NPs and VD3. The potential of CaCO_3 NP-based stabilized Pickering emulsion as an acid-responsive delivery system for food, and medical applications was also discussed.

Materials and methods

Materials

Food-grade calcium hydroxide slurry (8% w/w) was supplied by Enping Hui Xiang Industrial Co., Ltd. (Jiangmen, China). Medium-chain triglyceride (MCT; C8:C10 = 60:40) with a density of $0.943 \text{ g}\cdot\text{mL}^{-1}$ was purchased from Britz Networks Sdn. Bhd (Melaka, Malaysia) and used as received. Food additive grade commercial CaCO_3 powder (>99%), referred to as CCaCO_3 , was purchased from Jiarun Biotechnology (Henan, China). Tween 80 (TW80) was obtained from Aladdin (China, T104865). VD3 (cholecalciferol) (>98%) was obtained from Macklin (China, C804669). Enzymes and reagents used in simulated gastric and intestinal digestions were hydrochloric acid (Guangzhou Chemical Reagent Factory, China), pepsin (>400 U/mg; Sigma-Aldrich, USA, P7000), bile salt (Sigma-Aldrich, USA, 48,305), lipase (30–90 U/mg; Sigma-Aldrich, USA, L3126). Other reagents used included curmarin-6 (Cur-6; Aladdin, China, C100929), rhodamine B (RB; Aladdin, China, R104960), phosphate-buffer saline (PBS; Beyotime, China, C0221A), methanol (Merck, Germany, 106,007), methanesulfonic acid (Thermo, USA, 057558), and Nile red (Sigma-Aldrich, USA, 72,485). Ultrapure water was used in all experiments.

Pilot-scale preparation of CaCO_3 NPs

CaCO_3 NPs were synthesized by the gas-solid-liquid carbonation method (Fig. 1a) using a pilot-scale setup. CO_2 (15 L/min) was bubbled into 120 L of calcium hydroxide at an appointed concentration of 4% (w/v) in the

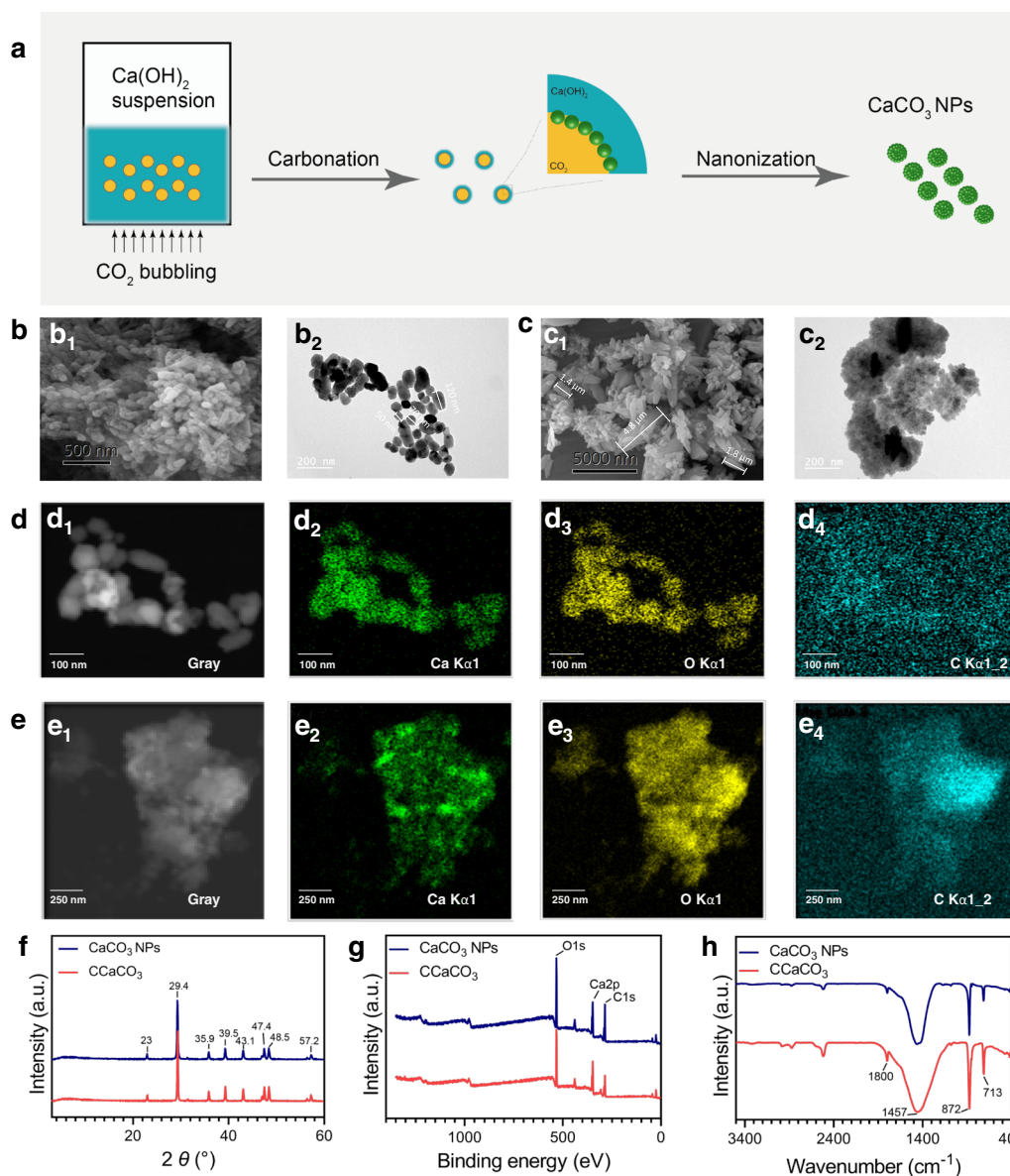


Fig. 1 Fabrication and structure/composition characterization of the CaCO_3 NPs and CCaCO_3 . **a** Schematic illustration of the fabrication process of the CaCO_3 NPs. SEM (**b₁** and **c₁**) and TEM (**b₂** and **c₂**) images of CaCO_3 NPs and CCaCO_3 , respectively. TEM/EDS elemental mapping images of the **d** CaCO_3 NPs and **e** CCaCO_3 . **f** XRD, **g** XPS, and **h** FTIR spectra of the CaCO_3 NPs and CCaCO_3

crystallizer to start the carbonation reaction under a controlled temperature of approximately $25 \pm 2^\circ\text{C}$ maintained by circulating water. The carbonation was kept for ~ 10 min until complete reaction was achieved, as verified by the decrease in system pH to approximately 7. For particle aging, the slurry was transferred to an open tank and stirred at 250 rpm for 12 h until the pH was stable at 7. Afterward, the suspension was centrifuged at 5,000 g for 20 min, vacuum-dried for 12 h, and ground to pass

through a 200-mesh screen. The pulverized powder was stored until further use.

Structural and morphologic characterization

The crystalline structure of CCaCO_3 and CaCO_3 NPs was measured using an Ultima IV X-ray diffractometer (XRD, Rigaku, Japan). X-ray photoelectron spectroscopy (XPS) measurements were carried out using a K-alpha⁺ spectrometer (Thermo Scientific, USA). Fourier transform infrared spectra (FTIR) of the samples were

measured using a Tensor 27 spectrometer (Bruker, Germany). Nanostructures of CaCO_3 NPs and CCaCO_3 were captured by a TECNAI G2 F20 transmission electron microscopy (TEM) (Phenom, the Netherlands). Samples were suspended into aqueous solutions and loaded onto a 200-mesh copper grid. Energy-dispersive X-ray spectroscopy (EDS)-mapping analyses were performed at several locations on the substrate to confirm the presence of calcium, oxygen, and carbon. Scanning electron microscopy (SEM) images were taken with a field emission scanning electron microscopy (LE, Phenom, the Netherlands). The samples were carefully mounted on a copper grid, which was stuck on double-sided carbon tape and sputter-coated with gold before scanning. The mean particle size of CaCO_3 NPs was measured and calculated using the Nano Measurer software (Version 1.2).

Preparation of the CaCO_3 NP-based stabilized emulsions

Preliminary experiments on the structural stability of the CaCO_3 NPs were conducted in aqueous solutions at pH=7.4, 6.8, and 5.3. According to TEM data (Additional file 1: Figure S1), surface erosion was evident for the CaCO_3 NPs at pH 5.3. This finding predicts CaCO_3 NP bulk disintegration at pH levels below 5.3 [11]. Since structural intactness is the basic prerequisite for a particle Pickering emulsifier, acidic pH conditions were not taken into account, and the emulsification performance of the CaCO_3 NPs was investigated at pH 7.4. Conveniently, weighted CaCO_3 NP powder was stirred into PBS (20 mmol·L⁻¹, pH 7.4) at a concentration (*c*) of 1–4% (w/v) and then passed through a UH-5 homogenizer (Union-Biotech Co., Ltd, Shanghai, China) equipped with a diamond-coated valve to disrupt the formed micron aggregates. The homogenization was conducted at 120 MPa for three passes. Sodium azide (0.02% w/v) was added as the preservative. The aqueous phase prepared above was mixed with MCT (to yield a total volume of 20 mL) at an oil volume fraction ($\phi = V_{\text{oil}} / (V_{\text{oil}} + V_{\text{water}})$) between 0.2 and 0.9, with an increment of 0.1. The two-phase mixture was homogenized by a handheld dispenser (Heidolph, SilentCrusher M, Germany) at 8,000 rpm for 2 min. The shearing condition was selected based on the trends of mean droplet size and droplet size distribution (DSD) with increasing shearing speed from 5,000 to 20,000 rpm (Additional file 1: Figure S2). In all emulsions, the *c* refers to the continuous phase rather than the whole emulsion. Emulsions were transferred to plastic tubes or screw-cap glass vials for measurements of mean droplet size ("Emulsion characterization" section), visual appearance, and microscopic observation ("Emulsion characterization" section) at set time intervals (0 and 30 days). Selected emulsions were stored at room temperature

(RT) and 4 °C for the characterization of emulsion stability. With CCaCO_3 or TW80 as emulsifiers, two control groups were set for comparison (Additional file 1: Figures S3 and S4). For these two control groups, shearing conditions (speed and time) were the same as those of the CaCO_3 NPs group.

Emulsion characterization

The DSD, Sauter mean diameter (d_{32}) [31], and specific surface area of the emulsion were measured using a Mastersizer 3000 particle sizer (Malvern, UK) with the refractive indexes of 1.33 and 1.45 for water and MCT, respectively. Bright field microscopic observations were carried out using an EVOS FL microscopy (ThermoFisher, USA). An aliquot of emulsion (5 μL) was carefully taken from each examined sample, pitted onto a glass slide, covered with a cover glass, and imaged under bright field mode. To visually evaluate the stability of emulsion often perceived as creaming, sediment, and demulsification into an oil layer, the emulsions were placed in plastic centrifugal tubes, and then their visual appearance was imaged by a digital camera. Storage and loss moduli of emulsions were measured using an AR1500EX rheometer (TA Instruments, USA) equipped with a parallel plate geometry (diameter: 40 mm, gap: 1 mm). A 1 mL emulsion was loaded onto the plate and covered with silicone oil around the edges of the sample to avoid solvent evaporation. All measurements were conducted at 25 °C. A set of emulsions ($\phi=0.8$) stabilized by TW80 at concentrations of 0.125–1% w/v served as control.

Centrifugation stability

Centrifugation stability measurement was performed on two representative emulsions stabilized by either CaCO_3 NPs or TW80 (control). Briefly, each tested emulsion (5 mL) was stored in a 15-mL screw-capped centrifuge tube and then centrifuged at 4000 *g* [32, 33] for 5 min. The centrifugal instability of emulsion was assessed based on the creaming index, which is calculated by the following equation [32].

$$\% \text{Creaming index} = \frac{H_s}{H_t} \times 100,$$

where H_s and H_t represent the height of the lower aqueous phase layer and the total height of the centrifuged emulsion.

Stability of emulsion upon dilution

Emulsion stability upon dilution and storage was studied for the CaCO_3 NPs stabilized emulsion ($\phi=0.8$, $c=4\%$ w/v) and for the TW80 control ($\phi=0.8$, $c=0.5\%$ w/v). Each emulsion type was freshly prepared and then separately diluted 2, 3, and 5 times with ultrapure water and

stored at RT for 7 days. Mean droplet diameter and DSD were measured for the two parent emulsions and their diluted emulsions before and after storage.

Preparation and characterization of VD3-encapsulated emulsion

The VD3 loaded Pickering emulsion was formulated with 14 g MCT oil containing 40 mg VD3 as the oil phase and 5.96 g of CaCO₃ NP suspension ($c=4\%$ w/v) to yield a total weight of 20 g and a VD3 concentration of 2.0 mg/g of the whole emulsion. A control group was specifically prepared in the same manner as that of CaCO₃ NPs except using TW80 ($c=0.5\%$ w/v) solution instead of CaCO₃ NPs dispersion as the continuous phase. A 2 mg/mL VD3 containing MCT oil was also used as a control group. Each sample to be tested was immediately transferred into screwed glass vials for avoiding excessive exposure to oxygen and then stored at 4 °C and RT. At the pre-designated time points, an aliquot (1 g) of the stored emulsion was withdrawn and then mixed with ethanol (1:9 by vol) with assisted vortexing (30 s) to extract VD3 and MCT from the emulsion. After centrifugation at 15,000 *g* for 15 min, the supernatant was diluted 10-fold with ethanol, passed through a 0.22 μm filter, injected into a high-performance liquid chromatography (HPLC) system equipped with an Atlantic T3-C18 column (4.6 × 250 mm, 5 μm, Waters, USA), and isocratically eluted by methanol at a flow rate of 1.0 mL/min. The quantification of VD3 was achieved using an ultraviolet (UV) detector (Agilent Technologies, USA) at 265 nm ($R^2=0.9999$). The content of the remaining VD3 was calculated accordingly to the following equation:

$$\% \text{ remaining VD3} = \frac{W_i}{W_0} \times 100,$$

where W_0 and W_i represent the total feeding weight of VD3 before storage and the remaining weight of VD3 after storage, respectively.

Simulated GI digestion

The digesting behaviors of VD3-loaded CaCO₃ NP-based stabilized emulsion ($\phi=0.8$, $c=4\%$ w/v) were studied using the two-stage *in vitro* digestion model based on previous research [34, 35] with slight modifications. A VD3-loaded TW80-stabilized emulsion ($\phi=0.8$, $c=0.5\%$ w/v) and a VD3 powder were used as controls. Assessment of the visual appearance and quantification of the VD3 content were performed at the end of the following two processes.

Gastric digestion. Briefly, the emulsion was diluted 40-fold with ultrapure water and then incubated in a water bath at 37 °C. Ten mL of the diluted and prewarmed emulsion (containing 0.18 g oil) was mixed with 10 mL

simulated gastric fluid (pH 1.2; 34 mmol·L⁻¹ NaCl, and 3.2 mg·mL⁻¹ pepsin) [36] in a 100 mL glass beaker; this mixture was adjusted to pH 2.5 using NaOH solutions and then incubated at 37 °C with stirring (1,000 rpm) for 1 h. At the end of digestion, a 250 μL aliquot sample was withdrawn from the aqueous phase for calcium quantification by the established HPIC procedure (Additional file 1: Figure S5), to which an equal volume of phosphate buffer was supplemented to the digestive fluid.

Intestinal digestion. The whole gastric digested mixture was adjusted to pH 7.0 and mixed with 1.5 mL of simulated intestinal fluid (containing 250 mM CaCl₂ and 3 M NaCl), and supplemented with 3.5 mL of bile salts (54 mg·mL⁻¹) [34]. After pH readjustment to 7.0, 2.5 mL of the lipase solution was added to start the lipolytic reaction at 37 °C for 2 h with constant stirring at 250 rpm. An autotitrator (Metrohm Ltd., USA) was used to monitor the pH during the whole digestion period and adjusted the pH back to 7.0 by titration with a 0.1 M NaOH solution. The amount of free fatty acids (FFA) produced by lipolysis based on its added volume into the reaction vessel was calculated by the following equation [35]:

$$\% \text{ FFA} = \frac{(C_{\text{NaOH}} \times V_{\text{NaOH}} \times M_{\text{wLipid}})}{(W_{\text{Lipid}} \times 2)} \times 100,$$

where C_{NaOH} is the molarity of the NaOH solution employed (0.1 M), V_{NaOH} (L) is the volume of NaOH required to neutralize FFA released, M_{wLipid} is the average molecular weight of MCT (503.9 g·mol⁻¹) calculated based on the C8: C10 proportion of MCT, and W_{Lipid} is the total weight of MCT (0.18 g) used for digestion.

Fluorescent microscopy

The microstructure of the emulsions after *in vitro* gastric and intestinal digestions was measured using fluorescent microscopy (EVOS FL, ThermoFisher, USA). All ingredients and their concentrations were the same as in "Simulated GI digestion" section except that the oily phase was stained with Nile red before emulsification. The dyed emulsion was treated in the same manner as "Simulated GI digestion" section. At each phase, the visual appearance of the digested emulsion was analyzed, and the emulsion microstructure was analyzed under red fluorescence imaging. To evidence the adsorption of CaCO₃ NPs onto oil droplets, we examined two selected emulsions ($\phi=0.8$) stabilized by CaCO₃ NPs ($c=4\%$ w/v) and TW80 ($c=0.5\%$ w/v), respectively, using a confocal laser scanning microscope (LSM 880 with AiryScan, Carl Zeiss). Before emulsification, the oil phase of both emulsions was dyed by Cur-6, while RB dyed the continuous phase containing CaCO₃ NPs. Fluorescence from Cur-6 and RB was excited at 458 nm and 543 nm, respectively.

Animal study and hematology analysis

The *in vivo* oral toxicity of CaCO₃ NPs stabilized emulsion was evaluated using a mouse model with the approval of the Laboratory Animal Ethics Committee of Jinan University. Four-week-old female ICR mice, purchased from GemPharmatech Co., Ltd. (Jiangsu, China), were randomly divided into four groups. Mice of the three treated groups were gavaged with the CaCO₃ NPs stabilized emulsion ($\phi=0.8$ and $c=4\%$ w/v) at daily doses of 325, 650, 1300 mg/kg (CaCO₃ dose), respectively, which equates to 1, 2, and 4 times of the daily calcium dose for adult as recommended by the National Institutes of Health (NIH). The mice of the control group received 0.9% NaCl per day. After 7-day gavage treatment, the mice were euthanized; blood samples were collected, centrifuged at 3000 rpm \times 15 min at 4 °C to obtain serum, and sent to Servicebio Biotechnology Co., Ltd (Wuhan, China) for hematological analysis. Besides, major organs were isolated, fixed in 4% paraformaldehyde, and stained with hematoxylin and eosin (H&E).

Statistical analysis

Unless otherwise stated, all data presented are the mean of three independent triplicates. Statistical evaluation was performed using the SPSS Statistics software (version 20.0, IBM Corp., USA). The difference between means was analyzed by a one-way analysis of variance (ANOVA)/Duncan's test ($p < 0.05$).

Results and discussion

Preparation and characterization of the CaCO₃ NPs

The as-prepared CaCO₃ NPs had an ellipsoidal geometry with sizes ranging from 40 to 140 nm, as analyzed by the SEM and TEM analyses (Fig. 1b). Similar morphologies have been reported for the CaCO₃ NPs [37]. In contrast, CCaCO₃ displayed amorphous structures of ununiform sizes, of which some had diameters greater than 1 μ m (Fig. 1c). The three constituent elements, namely Ca, O, and C, were distributed in both the CaCO₃ NPs and CCaCO₃ as analyzed by the EDS elemental mapping (Fig. 1d and e). Nevertheless, the C signal was negligible for the CaCO₃ NPs due to the background noise generated from the carbon supporting film of the copper grid. Quantification of the calcium content showed that calcium represented $39.4 \pm 0.9\%$ and $38.3 \pm 1.2\%$ of the CaCO₃ NPs and CCaCO₃ (Additional file 1: Figure S5), respectively, which agreed well with that of pure anhydrous calcium carbonate. The CaCO₃ NPs and CCaCO₃ exhibited similar X-ray diffraction patterns consisting of characteristic peaks at 29.4°, 35.9°, 43.1°, 47.4°, 48.5°, and 57.2° (Fig. 1f), which corresponded to calcite [38]. The XPS (Fig. 1g) and FTIR (Fig. 1h) analyses indicated structural similarity between the CaCO₃ NPs and CCaCO₃,

in which the CaCO₃ NPs and CCaCO₃ exhibited similar spectroscopic data. All of the results demonstrated the successful fabrication of nanoparticulate CaCO₃ with almost identical compositional and crystalline properties but different morphologies.

Preparation of the CaCO₃ NP-based stabilized emulsions

Although various oils, including soy, corn, olive oils, MCT, etc. can be solvents for VD3, it should be mentioned that MCT is more applicable to carry VD3 due to its oxidation stability [39]. As a result, any adverse effect of lipid oxidation on the stability of VD3 can be ruled out. Also, as an oil phase, MCT is readily soluble in ethanol (Additional file 1: Figure S6); thus, it offers the convenience of injecting the VD3 containing MCT-ethanol solution onto the C18 analytical column without solvent evaporation ("Preparation and characterization of VD3-encapsulated emulsion" section). For these reasons, MCT was selected as the preferred oily phase in this study.

Previous studies [3, 17–20] have indicated that the CaCO₃ NPs render the formation of O/W emulsion. Therefore, we evaluated the ability of the CaCO₃ NPs and CCaCO₃ to emulsify the system with a ϕ of 0.8. The two phases were homogenized upon mechanic shearing (schematically shown in Fig. 2a) in the presence of the CaCO₃ NPs rather than CCaCO₃. Hence, CCaCO₃ was incapable of forming an emulsion even after increasing the particle concentration to 4% w/v (Additional file 1: Figure S3a), where most of the CCaCO₃ remained in the lower aqueous phase, as evidenced under microscopy observation (Additional file 1: Figure S3b). Instead, the CaCO₃ NPs resulted in emulsion formation at $c=1-4\%$ (Fig. 2b), and all of the emulsions (except that prepared with $c=4\%$ w/v) creamed right after preparation for storage of 12 h at room temperature. For the three creamed emulsions, no CaCO₃ NPs were detectable at the bottom of their aqueous lower layers, indicating that CaCO₃ NPs stayed in the emulsified phase, probably adsorbing on oily surfaces. Notably, the emulsion with $c=4\%$ was gel-like, displaying self-supporting properties. To study the interfacial behaviors of CaCO₃ NPs at different concentrations, we measured the interfacial tensions between MCT and different CaCO₃ NPs dispersions (1–4% w/v; see Additional file 1: Figure S7). The results showed that the interfacial tension values decreased upon CaCO₃ NPs addition in a concentration-dependent manner. To gain insight into such a unique texture of the 'gelled' emulsion, we visualized the emulsions under optical microscopy. The microscopic results (Fig. 2c) showed that oil droplets of different sizes were well distributed in all of the emulsions, but those contained in the concentrated ($c=4\%$ w/v) emulsion were stuck to each other very firmly, forming a gel-like network that restricted oil droplet development (Fig. 2c₄) [40]. Through this densely packed

manner, the oil droplets exhibited difficulty in moving, thereby maintaining the hardly flowing emulsion. According to previous findings, the critical ϕ required to form a high internal phase emulsion (HIPE) was around 0.74 (maximum of 0.80), where a gel-like network was formed due to the solid concentration-related oil droplet flocculation [40–42]. The red fluorescence of the image identified the RB-dyed CaCO_3 NPs, and the overlapped fluorescence of RB (red fluorescence) and Cur-6 (green fluorescence) evidently showed the adsorption of CaCO_3 particles at the boundary of oil droplet (Fig. 2d). Decreasing d_{32} values, which ranged from 76 μm to 101.2 μm , were detected at increasing c for the emulsions (Fig. 2e). The four emulsions had similar monomodal droplet size distributions, though the peak positions slightly shifted to smaller sizes at higher c values (Fig. 2f). At a lower c of 0.5% w/v, CaCO_3 still did not form an emulsion, whereas CaCO_3 NPs only generated a thin emulsified layer located between the upper oily and lower aqueous phases (Additional file 1: Figure S3c).

Figure 3 shows the dependence of G' and G'' on the shearing frequency for the emulsions prepared at different c values. G' was always higher than G'' , irrespective of the c used, and both G' and G'' were proportional to c (Fig. 3a). Interestingly, the largest increment in either G' or G'' occurred at $c=3\%$ (Fig. 3c). Since the d_{32} values at concentrations of 2% and 3% w/v are similar, it should be the continuous phases affecting the viscoelasticity properties of emulsions. To support our supposition, we measured apparent viscosities for the four dispersions of CaCO_3 NPs. The results showed that the viscosity increased rapidly when c increased from 2 to 3% w/v (Additional file 1: Figure S8), probably due to particle aggregation. Therefore, based on these findings, we ascribe the sharp G' or G'' increments to the continuous phase's thickening. For TW80 emulsions in the control group, the G' also increased with increasing concentrations (Fig. 3b), but in a lower range. The G' measured with TW80 at 1% w/v was about one-tenth of that with 4% w/v CaCO_3 NPs (Fig. 3d). Emulsion viscosity/viscoelasticity has been well-demonstrated to be one of the affecting factors to emulsion stability against droplet coalescence [43, 44]. Based on these observations, the highest viscoelasticity with $c=4\%$ may result in the most optimal stability. The c was set 4% w/v in the following experiments based on the creaming and viscoelasticity data.

The performance of the CaCO_3 NPs as an emulsion stabilizing agent was observed within a wide range of $\phi=0.2$ to 0.9. The emulsions prepared at ϕ values lower than 0.5 creamed soon after preparation, and the creaming heights were proportional to ϕ (Fig. 4a). At $\phi=0.2$, parts of the upper creamed layer deposited after 12 h of standing at RT (Fig. 4a). Increasing ϕ to a higher range of 0.7–0.8 resulted in stable emulsions based on the absence of creaming even after storage for 30 days (data not shown). Notably, self-standing properties were imparted into the emulsions prepared at $\phi=0.7$ –0.8. Further increasing ϕ up to 0.9, however, resulted in the presence of an emulsified layer as the lower phase, while most of the oily phase remained unemulsified. Microscopic data showed that the oil droplets were densely packed within the two HIPEs ($\phi=0.7$ –0.8), whereas relatively small-sized droplets were present in low ϕ emulsions ($\phi=0.3$ –0.6) (Fig. 4b). Analysis of the droplet characteristics further showed that the d_{32} values increased with increasing ϕ (Fig. 4c). The DSD patterns were nearly monomodal across a rather wide size ranging from 10s to 100s of μm (Fig. 4d). Based on the results of Fig. 4, it was concluded that emulsions of different droplet characteristics, specifically the droplet size and distribution could be fabricated by simply varying ϕ .

Centrifugation and dilution stability

Creaming is one of the emulsion-breaking mechanisms. In this study, both creamed and uncreamied emulsions were prepared, depending on the ϕ used (Fig. 4). To further analyze the creaming stability, we centrifuged the uncreamied one ($\phi=0.8$, $c=4\%$ w/v) at 4000 g for 5 min. For comparison, a 0.5% w/v TW80 stabilized emulsion was prepared at the same ϕ and treated in the same manner. As shown in Fig. 5a, each of the initial uncreamied emulsions separated into two phases after centrifugation, but no sedimentation occurred. No significant difference in creaming index was observed for the two examined emulsions (Fig. 5b).

Concentrated emulsions usually need to be diluted into thin forms before use. Emulsion dilution, nevertheless, may destabilize the stability of the droplets. Hence, it is of significance to investigate the dilution stability of high internal phase Pickering and traditional emulsions.

(See figure on next page.)

Fig. 2 Preparation and characterization of the Pickering emulsions stabilized by the CaCO_3 NPs. **a** Schematic illustration of the fabrication process of the CaCO_3 NP-based stabilized Pickering emulsion. **b** Visual appearance of creamed and homogenous emulsions ($c=1$ –4% w/v and $\phi=0.8$). The right panel shows the gel-like emulsion prepared with the highest c (4% w/v). **c** Micrographic images showing the microstructure of emulsions, as presented in **b**. Scale bars are 200 μm . **d** Confocal laser scanning microscope images of droplets stabilized by CaCO_3 NPs. The oil droplet dyed by Cur-6 showed green fluorescence, whereas the CaCO_3 NPs dyed by RB showed red fluorescence. The scale bar is 30 μm . **e, f** Mean droplet diameter (d_{32}) and DSD of CaCO_3 NPs stabilized emulsions as a function of c . The particle concentration refers to the particles or surfactant concentration in the continuous phase rather than the whole emulsion. Data are mean \pm standard deviation in triplicate. Bars with different letters (a, b, and c) indicate statistically significant ($p < 0.05$) differences among samples

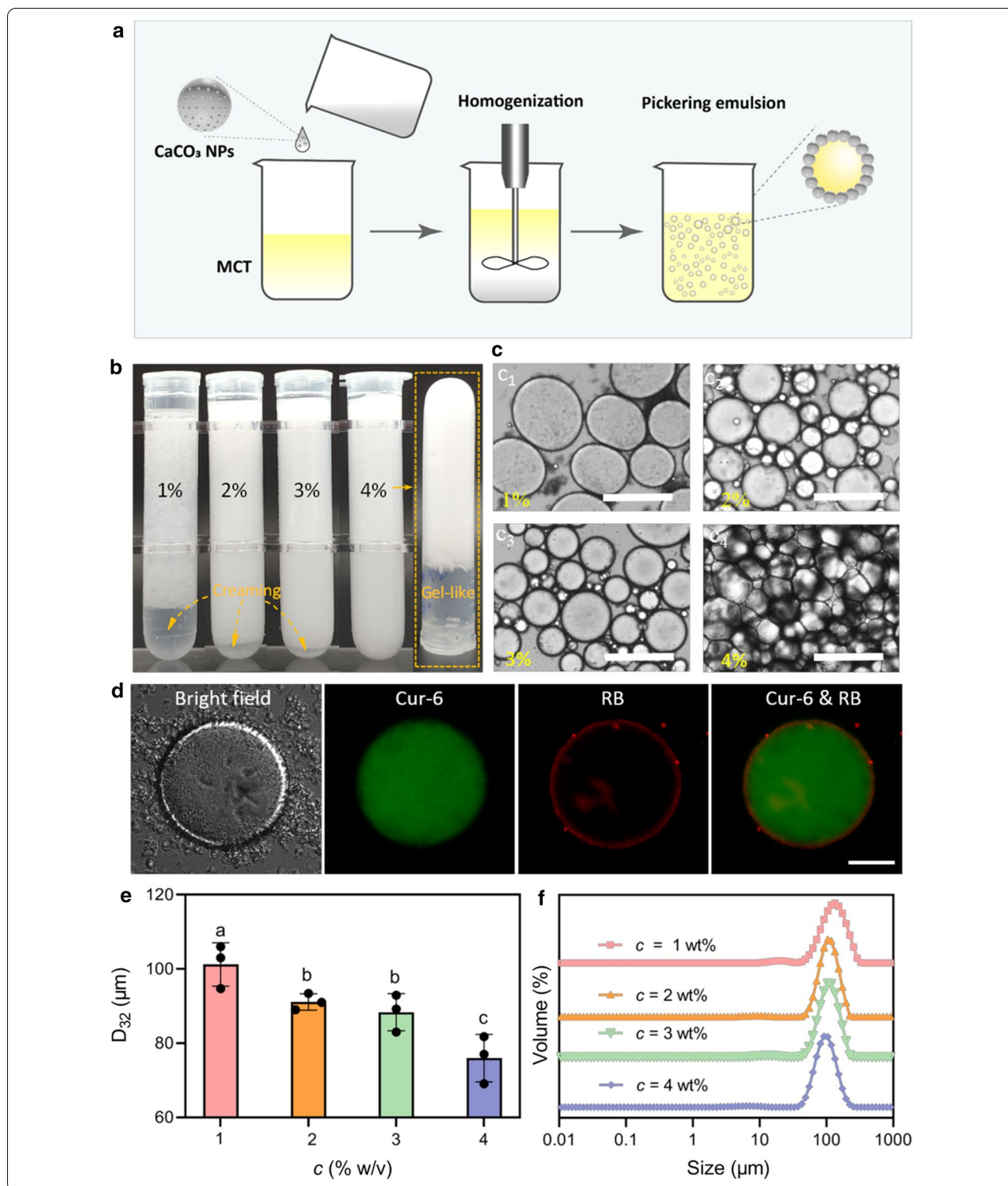
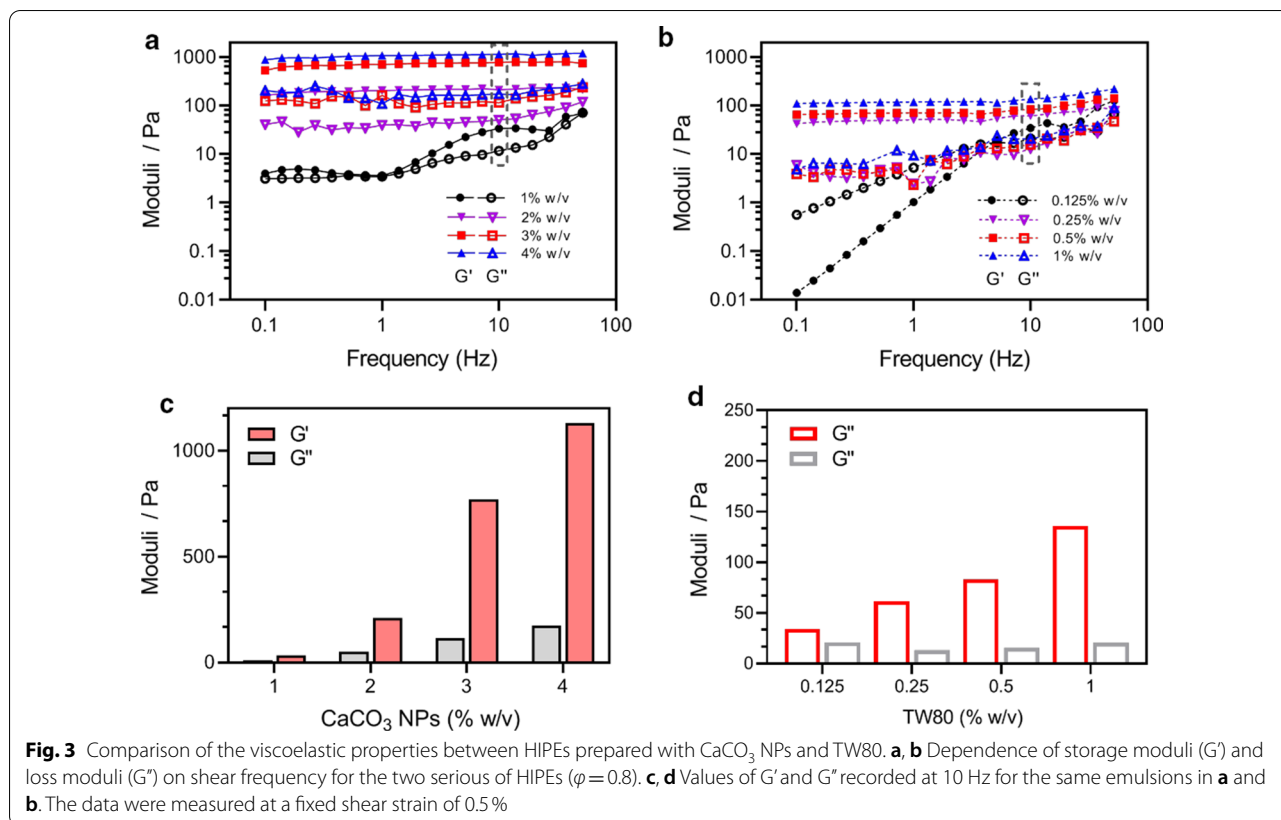


Figure 5c shows the effect of dilution of CaCO₃ NPs-stabilized Pickering emulsions and TW80-stabilized traditional emulsions on creaming and droplet characteristics. When diluted 2- to 5-folds, the emulsions

stabilized by CaCO₃ NPs soon stratified after 12 h at RT. What's more, the lower aqueous phase's height was proportional to the dilution ratio used. In contrast, the TW80 control group's diluted emulsions were not layered



within 12 h because the stratification was too slow to render apparent phase separation. After 7-day storage, the diluted TW80 emulsions stratified dramatically. Despite the occurrence of stratification, dilution (2- to 5-folds) and storage time (7 d) had no apparent effects on the shapes of droplets and mean diameters (Fig. 5d–h). Hence, CaCO₃ NPs-stabilized Pickering emulsions and TW80-stabilized traditional emulsions showed comparable and satisfying dilution stability.

Encapsulation of VD3

HIPE shows great promise as an effective delivery system because it stabilizes a high volume of oily phase that is compatible with lipophilic substances. Encouraged by the desired stability of CaCO₃ NP-based stabilized HIPE ($\phi=0.8$), we exploited it as a delivery vehicle for lipophilic compounds using VD3 as a model substance (Fig. 6a) and analyzed the remaining percentage of the encapsulated VD3 (Fig. 6b) at 4 °C and RT. For a fair comparison, VD3 was not only dissolved in MCT oil alone but also loaded in the TW80 stabilized emulsion at the same concentration, and then both these two VD3-containing samples were processed in the same manner as the CaCO₃ NPs group. The results showed VD3 contents of the three groups did not decrease significantly after

30-day storage at 4 °C. However, when stored at RT for 30 days, the content of remaining VD3 was significantly reduced to $90.5 \pm 2.8\%$ for MCT and $88.9 \pm 0.7\%$ for the TW80 control, respectively, in contrast to no significant decrease in VD3 ($p > 0.05$) in the CaCO₃ NPs group. It could be therefore calculated that about 10% of VD3 loss occurred in the two control groups, which could be due to oxidative degradation [2]. For the CaCO₃ NPs group, the remaining percentage of VD3 remained unchanged after storage at RT. An analysis of mean droplet size also confirmed the stability of the stored emulsions (Additional file 1: Figure S9). A comparison of the VD3 retention percentage revealed that the emulsified MCT oil environment ($\phi=0.8$) did not necessarily protect VD3 against degradation during the 30-day period. It is worth noting that the emulsion with a larger mean droplet size, in turn, results in a smaller specific surface area, and vice versa. Therefore, the high loss of VD3 in the TW80-stabilized emulsion may partially correspond to its higher specific surface area ($385.1 \pm 26.2 \text{ m}^2/\text{kg}$ of the TW80 group versus $95.9 \pm 14.3 \text{ m}^2/\text{kg}$ of the CaCO₃ NPs group). It has been proposed that viscosity could affect oxidation by reducing the diffusion of potential oxidizing substances [45]. Considering the dramatic difference in viscosity

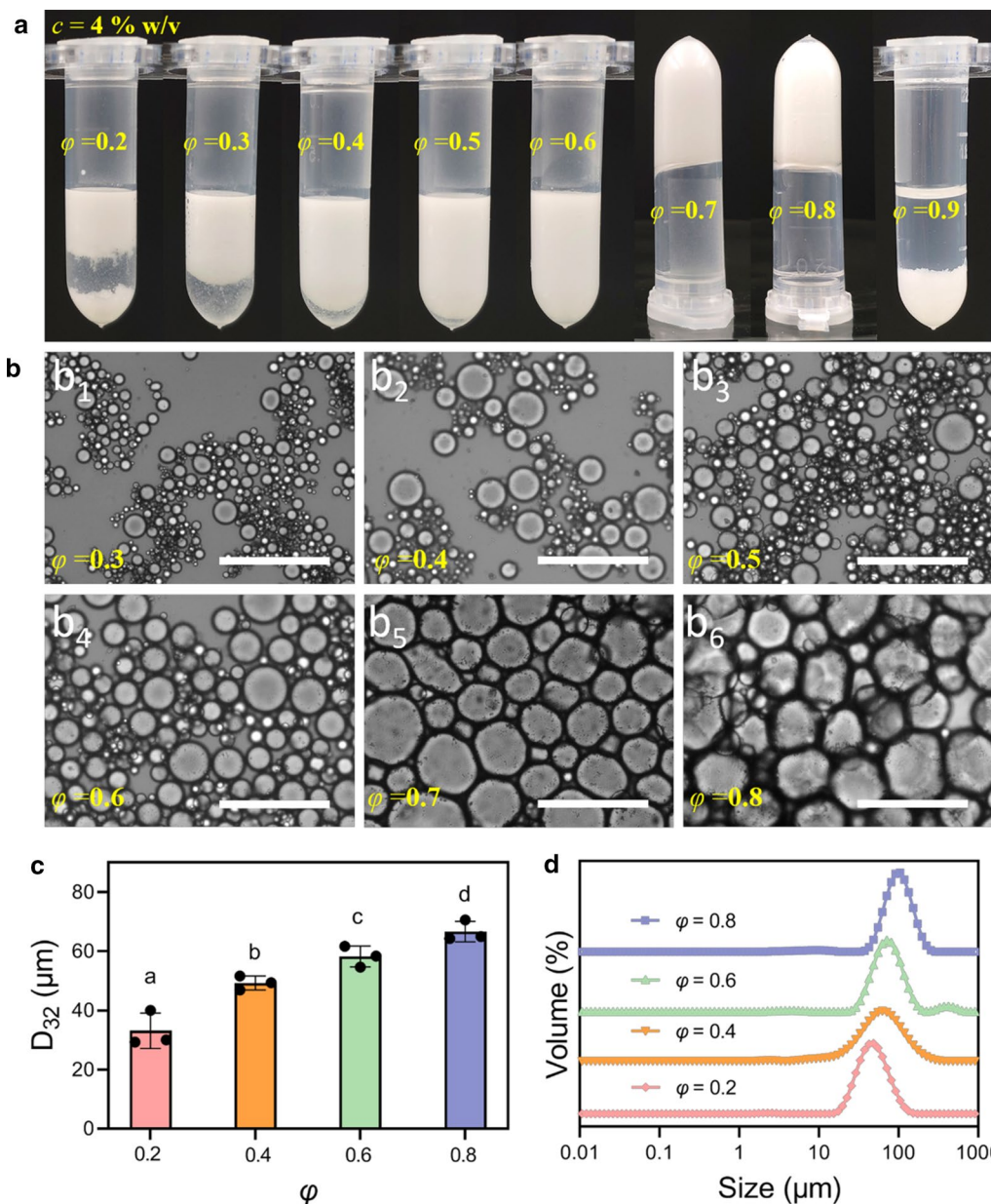
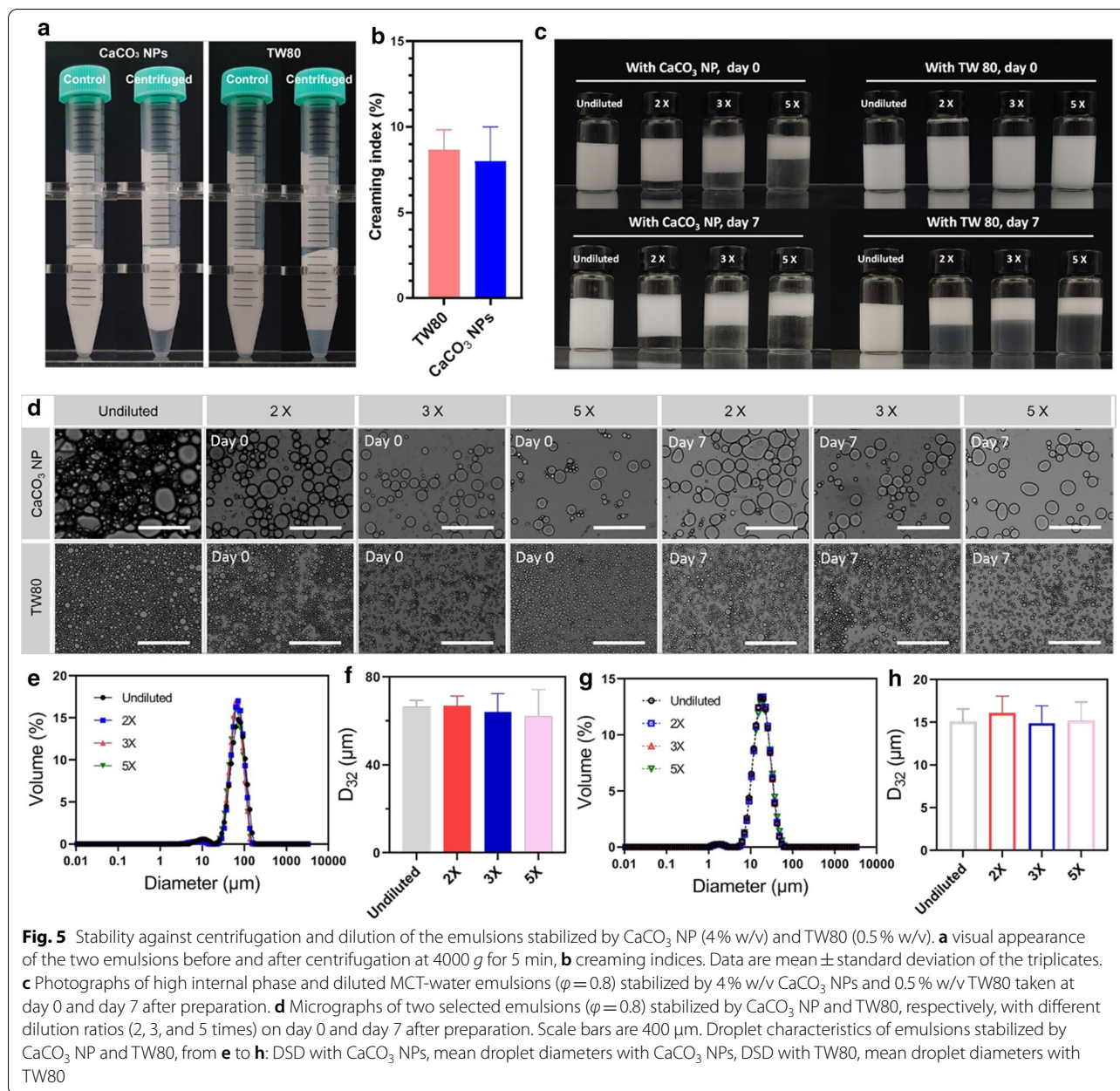


Fig. 4 CaCO₃ NP-based stabilized Pickering emulsion displayed ϕ -dependent emulsification properties. **a** Visual appearance of emulsions ($c = 4\% \text{ w/v}$) with ϕ ranging from 0.2 to 0.9. Samples were placed into vials just after preparation and then photos were taken after standing at room temperature for 12 h. **b** Micrographic images of the six representative emulsions ($c = 4\% \text{ w/v}$ and $\phi = 0.3\text{--}0.8$). Scale bars: 200 μm . **c, d** d_{32} and DSD of the selected emulsions with ϕ increment of 0.2, between 0.2 and 0.8. Data are mean \pm standard deviation of the triplicates. Bars with different letters (a, b, c, and d) indicate statistically significant ($p < 0.05$) different samples

between the TW80- and CaCO₃ NPs stabilized emulsions (Fig. 3), we assume that the higher viscosity of the CaCO₃ NPs stabilized emulsion is partially responsible for the enhanced stability of VD3 through reducing the diffusion of oxidizing factors (e.g., oxygen).

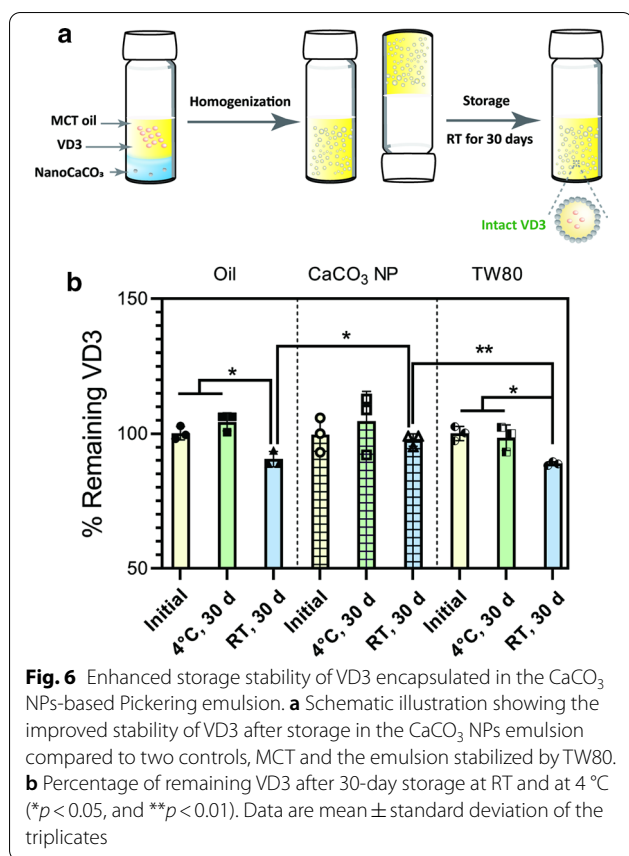
Responsiveness of the CaCO₃ NP-based Pickering emulsion under simulated in vitro GI conditions

For an edible Pickering emulsion formulation, it is necessary to understand the digestibility in the GI tract. Hence, we performed simulated in vitro gastric and intestinal digestions to highlight the fate of the VD3-loaded CaCO₃ NPs stabilized Pickering emulsion (depicted by the



schematic, as shown in Fig. 7a). Analysis of visual appearance was first carried out to show that the demulsification suffered in the simulated gastric fluid (pH 2.5). Upon digestion by acid, emulsion droplets stabilized by CaCO₃ NPs rather than TW80 (Fig. 7e) coalesced into a bulk upper oil phase (Fig. 7f) because the CaCO₃ NPs initially adsorbed onto the oil droplet surface were completely decomposed into Ca²⁺, as verified by the quantification analysis of Ca²⁺ (Fig. 7b). Similar demulsification by acid has been reported for emulsions stabilized by hydroxyapatite or calcium

phosphate particles [11, 12]. From the standpoint of dietary calcium, such acid-responsive disintegration of the CaCO₃ NPs would be an effective means for providing Ca²⁺ for physiological use. After gastric digestion at a neutral pH (7.4), the demulsified oil phase was depleted by the simulated intestinal fluid after 2-h digestion. The total percentage of FFA released was estimated to be 85.7 ± 8.7% and 105.7 ± 4.1% for the nano CaCO₃- and TW80-stabilized emulsions, respectively, based on their cumulative releases of FFA (Fig. 7c). Considering the result obtained in this work, calcium ions that were liberated from the stabilizing



CaCO₃ NPs to the intestinal fluid may, on the one hand, decrease the FFA content because they may retard the micellization of oil during lipolysis and, on the other hand, form precipitates with free fatty acids [28]. When used as a delivery vehicle ingested orally, maintaining a satisfactory percentage of cargo remaining after the GI tract would be significant to predict the bioavailability of the cargo. For this reason, changes in the VD3 content were analyzed for the representative HIPE ($\phi=0.8$) when treated by gastric and intestinal digestion. The result showed that VD solubilized in the hydrolysate decreased to $79 \pm 3.3\%$ and $72.8 \pm 4.1\%$ for the CaCO₃ NPs stabilized emulsion after stepwise gastric and intestinal digestions, respectively, and $96.2 \pm 2.3\%$ and $83.3 \pm 2.3\%$ for the TW80 stabilized emulsion (Fig. 7d). VD3 appeared to be better protected by the TW80 emulsion from degradation by gastric acid, which may be related to the stability in the gastric fluid (Fig. 7e). During the intestinal digestion, the oil phase of the TW80 emulsion was digested more thoroughly (Fig. 7c), which may promote the micellization of oil and VD3. In both cases, although the loss of one part of VD3 did take place, the final remaining percentage of VD3 was much higher with comparison to the control sample (VD3 powder) which presented a value of $19.6 \pm 1.4\%$ (Fig. 7d). These

quantitative results concerning Ca²⁺ and VD3 indicate that the VD3-containing HIPE may be useful as a calcium/VD3-fortified Pickering formulation.

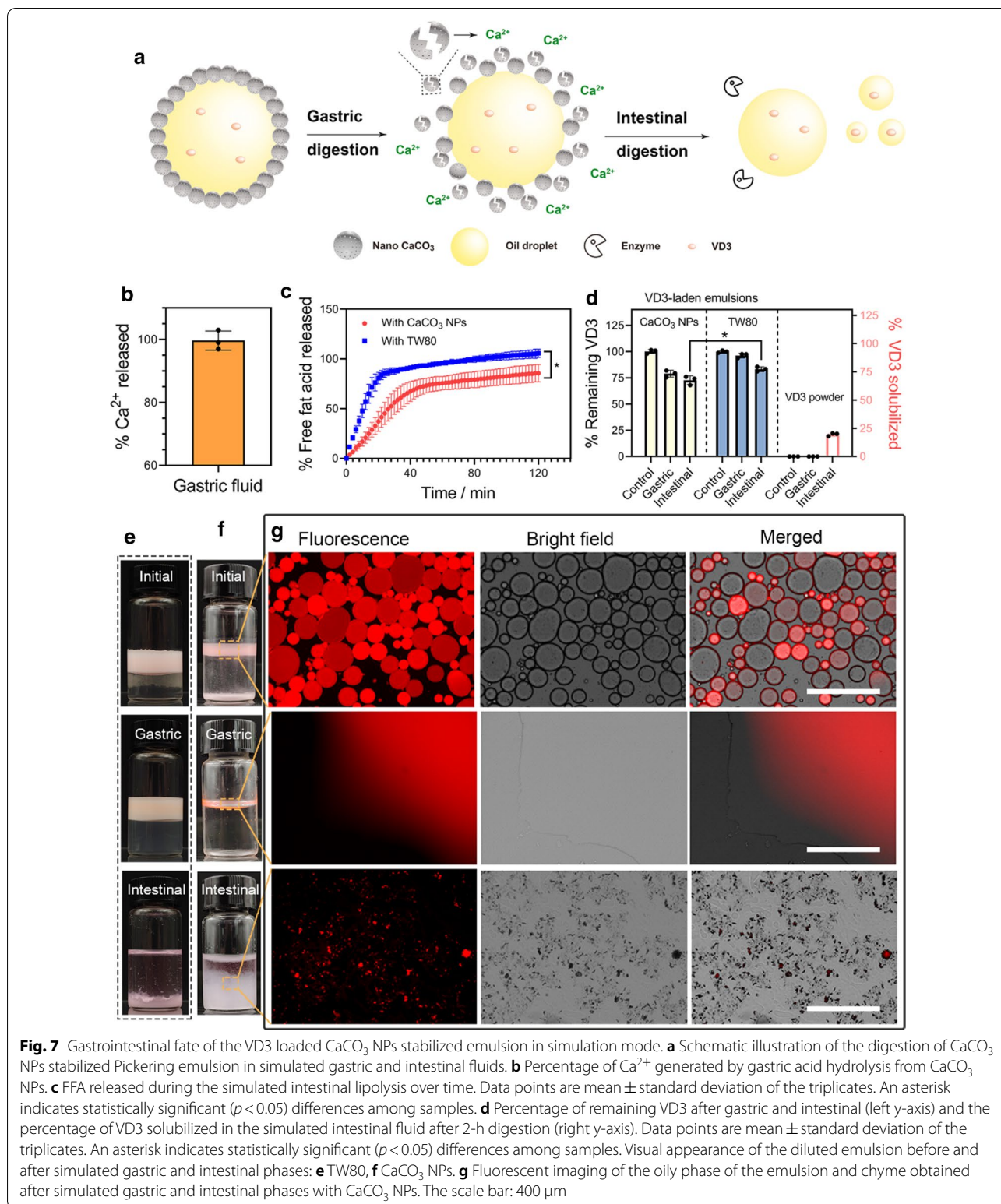
To microscopically detail the demulsification process with CaCO₃ NPs in simulated GI conditions (Fig. 7f g), we characterized the dispersed oil component using fluorescent microscopy. Initially, micrometered oil droplets bearing red fluorescence were clearly imaged. (Fig. 7f), which were digested into small fragments in the following simulated intestinal environment. This result indicated that the oil layer was partially broken into small-sized droplets during the intestinal digestion process [46].

Oral toxicity assessment of CaCO₃ NPs stabilized emulsion in vivo

As a carrier for VD3 for oral administration, the safety of the CaCO₃ NPs stabilized MCT-water emulsion should be a primary concern. Hence, we conducted analyses of histopathology and blood biochemistry to study the in vivo toxicity due to the oral administration of CaCO₃ NPs stabilized emulsion. The results showed no pathological difference in the heart, liver, spleen, lungs, and kidneys between the three treated and control groups (Fig. 8A). Also, the safety of the CaCO₃ NPs stabilized emulsion was supported by the blood indices, including creatine kinase (CK), lactate dehydrogenase (LDH), alanine aminotransferase (ALT), aspartate aminotransferase (AST), albumin (ALB), blood urea nitrogen (BUN), uric acid (UA), and creatinine (CREA) (a–h in Fig. 8B). Interestingly, no difference in the four blood fat indicators (i.e., triglycerides: TG, cholesterol: CHO, high-density lipoprotein: HDL, and low-density lipoprotein: LDL, i–l in Fig. 8B) occurred between treated and control groups, indicating the intake of MCT during the administration of CaCO₃ NPs stabilized emulsion caused no additional burden to blood fat. Although a more extended period is required to systematically evaluate the toxicity of the CaCO₃ NPs stabilized emulsion, the promising results of the current short-term toxicity assessment (Fig. 8) suggest that this type of CaCO₃ NPs stabilized emulsions is of low toxicity and has potential food, pharmaceutical, and biomedical applications.

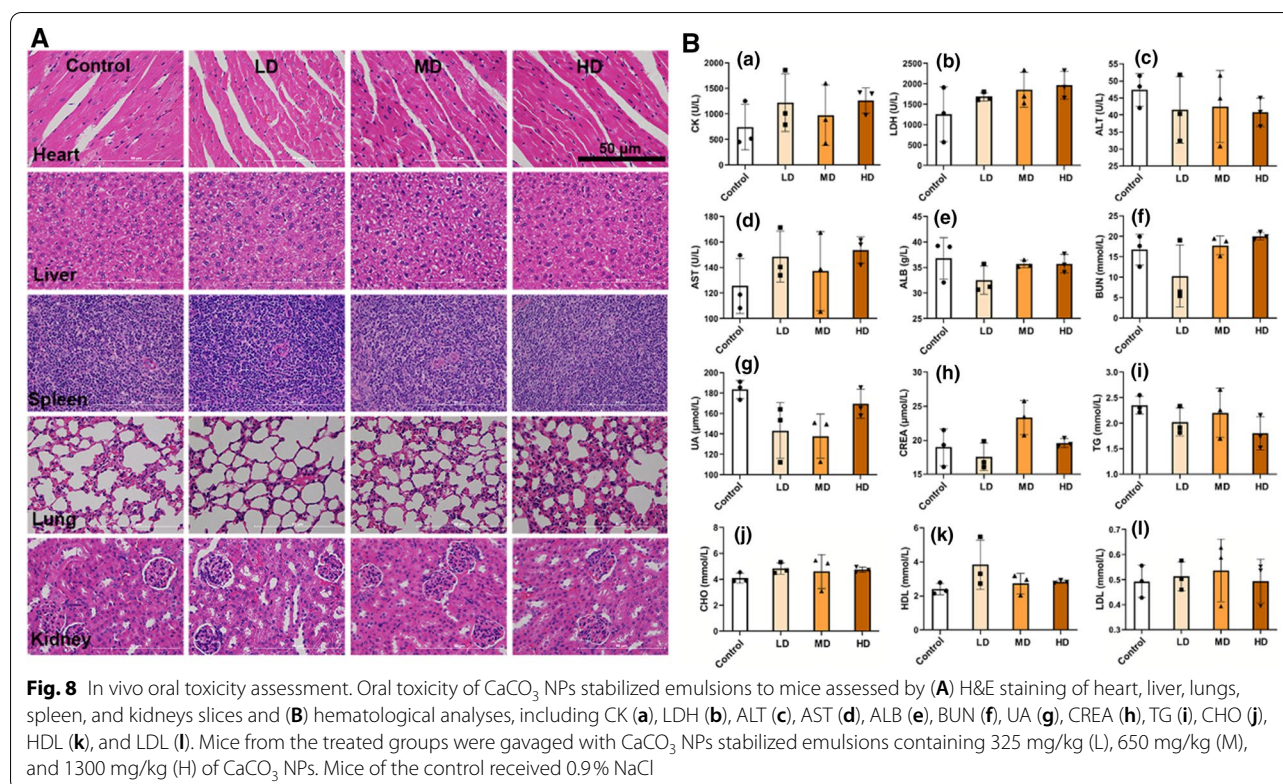
Conclusions

In summary, in this study, we prepared a type of bioreponsive CaCO₃ NP-based Pickering emulsion with drug-delivering and calcium-fortifying properties. This emulsion design can overcome the drawbacks of a physical blend of CaCO₃ NPs and VD3 and achieve the following advantages: (i) The stabilizing CaCO₃ NPs robustly protect the emulsified droplet against coalescence, which enhances the stored stability of the encapsulated VD3. (ii) The surface-adsorbed CaCO₃ NP layer results in the



release of Ca^{2+} and gastric acid-triggered demulsification after exposure to simulated gastric fluid, which favors subsequent lipolysis in the following intestinal phase. (iii)

The digestion of oil into FFA induces the release of VD3, which probably synergistically enhances the absorption rate of calcium. Together, this study not only provides



a type of Pickering emulsion-based encapsulation and delivery system by using CaCO₃ NPs as the emulsifier and MCT as the internal phase but also sheds light on the usage of the CaCO₃ NP-based stabilized Pickering emulsions for an edible purpose, particularly as calcium-fortified Pickering emulsions.

Supplementary Information

The online version contains supplementary material available at <https://doi.org/10.1186/s12951-021-00807-6>.

Additional file 1: Figure S1. Morphological change of the CaCO₃ NPs after exposure to different pH conditions for 30 min. **Figure S2.** Mean droplet diameter, droplet size distribution, and micrographic of CaCO₃ NP- and TW80-stabilized emulsions prepared under different shearing speeds. **Figure S3.** Insufficient emulsification performance of CaCO₃ and CaCO₃ NPs at different concentrations. **Figure S4.** MCT/water emulsions fabricated with TW80 at different parameters. **Figure S5.** Calcium contents of the CaCO₃ NPs and CaCO₃. **Figure S6.** Immiscibility of MCT and different oils and the separation of MCT and VD3 on a C18 column. **Figure S7.** Interfacial tension between the MCT/water interface decreased upon the addition of CaCO₃ NPs or TW80. **Figure S8.** Shear viscosity of CaCO₃ NPs dispersions at different concentrations. **Figure S9.** Changes in mean droplet diameter before and after storage at RT for 30 days.

Abbreviations

GRAS: Generally regarded as safe; VD3: Vitamin D3; MCT: Medium-chain triglyceride; TW80: Tween 80; Cur-6: Curcumin-6; RB: Rhodamine B; GI: Gastro-intestinal; PBS: Phosphate-buffer saline; XRD: X-ray diffractometer; XPS: X-ray photoelectron spectroscopy; FTIR: Fourier transform infrared spectra; TEM: Transmission electron microscopy; EDS: Energy-dispersive X-ray spectroscopy;

SEM: Scanning electron microscopy; HPLC: High-performance liquid chromatography; UV: Ultraviolet; FFA: Free fatty acids; NIH: National institutes of health; H&E: Hematoxylin and eosin; ANOVA: One-way analysis of variance; HIPE: High internal phase emulsion; CK: Creatine kinase; LDH: Lactate dehydrogenase; ALT: Alanine aminotransferase; AST: Aspartate aminotransferase; ALB: Albumin; BUN: Blood urea nitrogen; UA: Uric acid; UREA: Urea; CREA: Creatinine; TG: Triglycerides; CHO: Cholesterol; HDL: High-density lipoprotein; LDL: Low-density lipoprotein.

Acknowledgements

Not applicable.

Authors' contributions

XG and XL participated in experiments, data analysis, and manuscript writing, and contributed equally in this investigation; LC carried out experiments, and collected and analyzed data; WH carried out experiments; TC supervised the entire project and involved in the designing of conceptual framework and wrote the manuscript. All authors read and approved the final manuscript.

Funding

This work was supported by National Natural Science Foundation of China (21877049), Major Program for Tackling Key Problems of Industrial Technology in Guangzhou (201902020013), China Postdoctoral Science Foundation (2019M653279), Dedicated Fund for Promoting High-Quality Marine Economic Development in Guangdong Province (GDOE-2019-A31, 2020-035), Guangzhou Key Laboratory of Molecular and Functional Imaging for Clinical Translation (201905010003), Innovation Team Project in Guangdong Colleges and Universities (2019KCXTD008, 2019KTSX012), Opening fund of Hubei Key Laboratory of Bioinorganic Chemistry & Materia Medica (BCMM202001), the Open Fund of the Key Laboratory of Functional Molecular Engineering of Guangdong Province (2017KF06), Pearl River Nova Program of Guangzhou (201906010077) and Applications and K. C. Wong Education Foundation.

Availability of data and materials

All data generated or analyzed during this study are included in this article.

Ethics approval and consent to participate

The study had animal ethics approval from Jinan University Animal Ethics Committee. The manuscript does not contain clinical studies or patient data.

Consent for publication

All authors consent to publish.

Competing interests

The authors declared no competing financial interest.

Received: 29 November 2020 Accepted: 15 February 2021

Published online: 04 March 2021

References

- Harman CLG, Patel MA, Guldin S, Davies G-L. Recent developments in Pickering emulsions for biomedical applications. *Curr Opin Colloid Interface Sci.* 2019;39:173–89.
- Xiao J, Li Y, Huang Q. Recent advances on food-grade particles stabilized pickering emulsions: fabrication, characterization and research trends. *Trends Food Sci Technol.* 2016;55:48–60.
- Zhu Y, Lu LH, Gao J, Cui ZG, Binks BP. Effect of trace impurities in triglyceride oils on phase inversion of Pickering emulsions stabilized by CaCO₃ nanoparticles. *Colloids Surf A Physicochem Eng Asp.* 2013;417:126–32.
- Marto J, Ascenso A, Simoes S, Almeida AJ, Ribeiro HM. Pickering emulsions: challenges and opportunities in topical delivery. *Expert Opin Drug Deliv.* 2016;13:1093–107.
- Chen Y, Wei W, Zhu Y, Luo J, Liu R, Liu X. Synthesis of temperature/pH dual-stimuli-response multicompartmental microcapsules via pickering emulsion for preprogrammable payload release. *ACS Appl Mater Interfaces.* 2020;12:4821–32.
- Farinmade A, Ojo OF, Trout J, He J, John V, Blake DA, Lvov YM, Zhang D, Nguyen D, Bose A. Targeted and stimulus-responsive delivery of surfactant to the oil–water interface for applications in oil spill remediation. *ACS Appl Mater Interfaces.* 2020;12:1840–9.
- Tikekar RV, Pan Y, Nitin N. Fate of curcumin encapsulated in silica nanoparticle stabilized Pickering emulsion during storage and simulated digestion. *Food Res Int.* 2013;51:370–7.
- Mao L, Miao S. Structuring food emulsions to improve nutrient delivery during digestion. *Food Eng Rev.* 2015;7:439–51.
- Wei Y, Tong Z, Dai L, Wang D, Lv P, Liu J, Mao L, Yuan F, Gao Y. Influence of interfacial compositions on the microstructure, physicochemical stability, lipid digestion and β -carotene bioaccessibility of Pickering emulsions. *Food Hydrocoll.* 2020;104:105738.
- Dong Z, Feng L, Zhu W, Sun X, Gao M, Zhao H, Chao Y, Liu Z. CaCO₃ nanoparticles as an ultra-sensitive tumor-pH-responsive nanoplatfrom enabling real-time drug release monitoring and cancer combination therapy. *Biomaterials.* 2016;110:60–70.
- Fujii S, Okada M, Furuzono T. Hydroxyapatite nanoparticles as stimulus-responsive particulate emulsifiers and building block for porous materials. *J Colloid Interface Sci.* 2007;315:287–96.
- Ruan Q, Guo J, Wan Z, Ren J, Yang X. pH switchable Pickering emulsion based on soy peptides functionalized calcium phosphate particles. *Food Hydrocoll.* 2017;70:219–28.
- Tavernier I, Wijaya W, Van der Meeren P, Dewettinck K, Patel AR. Food-grade particles for emulsion stabilization. *Trends Food Sci Technol.* 2016;50:159–74.
- Sharma S, Verma A, Teja BV, Pandey G, Mittapelly N, Trivedi R, Mishra PR. An insight into functionalized calcium based inorganic nanomaterials in biomedicine: Trends and transitions. *Colloids Surf B.* 2015;133:120–39.
- Saad S, Kaur H, Natale G. Scalable chemical synthesis route to manufacture pH-responsive janus CaCO₃ micromotors. *Langmuir.* 2020;36:12590–600.
- Vavrusova M, Skibsted LH. Calcium nutrition. *Bioavail Fortif LWT.* 2014;59:1198–204.
- Binks BP, Muijlwijk K, Koman H, Poortinga AT. Food-grade Pickering stabilisation of foams by in situ hydrophobisation of calcium carbonate particles. *Food Hydrocoll.* 2017;63:585–92.
- Liu X, Wang L, Li B, Li J, Wei X. O/W Pickering emulsions stabilized by CaCO₃ and particle size effect. *Food Mach.* 2019;35:20–5.
- Cui ZG, Shi KZ, Cui YZ, Binks BP. Double phase inversion of emulsions stabilized by a mixture of CaCO₃ nanoparticles and sodium dodecyl sulphate. *Colloids Surf A Physicochem Eng Asp.* 2008;329:67–74.
- Huang F, Liang Y, He Y. On the Pickering emulsions stabilized by calcium carbonate particles with various morphologies. *Colloids Surf A Physicochem Eng Asp.* 2019;580:123722.
- Yang Y, Fang Z, Chen X, Zhang W, Xie Y, Chen Y, Liu Z, Yuan W. An overview of Pickering emulsions: solid-particle materials, classification, morphology, and applications. *Front Pharmacol.* 2017;8:287.
- Tari G, Ferreira JMF. Colloidal processing of calcium carbonate. *Ceram Int.* 1998;24:527–32.
- Lee J, Jo SH, Lim J. Effect of surface modification of CaCO₃ nanoparticles by a silane coupling agent methyltrimethoxysilane on the stability of foam and emulsion. *J Ind Eng Chem.* 2019;74:63–70.
- Erfanian A, Rasti B, Manap Y. Comparing the calcium bioavailability from two types of nano-sized enriched milk using in-vivo assay. *Food Chem.* 2017;214:606–13.
- Choi H-S, Han J, Chung S, Hong Y-H, Suh HJ. Nano-calcium ameliorates ovariectomy-induced bone loss in female rats. *Korean J Food Sci Anim Resour.* 2013;33:515–21.
- Ozturk B, Argin S, Ozilgen M, McClements DJ. Nanoemulsion delivery systems for oil-soluble vitamins: Influence of carrier oil type on lipid digestion and vitamin D3 bioaccessibility. *Food Chem.* 2015;187:499–506.
- Walia N, Dasgupta N, Ranjan S, Chen L, Ramalingam C. Fish oil based vitamin D nanoencapsulation by ultrasonication and bioaccessibility analysis in simulated gastro-intestinal tract. *Ultrason Sonochem.* 2017;39:623–35.
- Dima C, Dima S. Bioaccessibility study of calcium and vitamin D3 co-microencapsulated in water-in-oil-in-water double emulsions. *Food Chem.* 2020;303:125416.
- El-Boshy M, Refaat B, Almaimani RA, Abdelghany AH, Ahmad J, Idris S, Almasmoum H, Mahbub AA, Ghaith MM, BaSalamah MA. Vitamin D3 and calcium cosupplementation alleviates cadmium hepatotoxicity in the rat: Enhanced antioxidative and anti-inflammatory actions by remodeling cellular calcium pathways. *J Biochem Mol Toxicol.* 2020;34:e22440.
- Weinstein R, Haynes S, Zhao Y, Hickson E, Linden J, St. Pierre P, Ducharme P, Sulmasy P, Graves M, Bailey JA, et al. A liquid calcium + vitamin D3 supplement is effective prophylaxis against hypocalcemic toxicity during apheresis platelet donation. *J Clin Apher.* 2018;33:60–4.
- Kowalczyk PB, Drzymala J. Physical meaning of the Sauter mean diameter of spherical particulate matter. *Part Sci Technol.* 2016;34:645–7.
- Gong X, Wang Y, Chen L. Enhanced emulsifying properties of wood-based cellulose nanocrystals as Pickering emulsion stabilizer. *Carbohydr Polym.* 2017;169:295–303.
- Xiao J, Zhang M, Wang W, Li S, Wang Y, Du G, Zhang K, Li Y. Using Flammulina velutipes derived chitin-glucan nanofibrils to stabilize palm oil emulsion: A novel food grade Pickering emulsifier. *Int J Biol Macromol.* 2020;164:4628–37.
- Espinal-Ruiz M, Restrepo-Sánchez L-P, Narváez-Cuenca C-E, McClements DJ. Impact of pectin properties on lipid digestion under simulated gastrointestinal conditions: comparison of citrus and banana passion fruit (*Passiflora tripartita* var. *mollissima*) pectins. *Food Hydrocoll.* 2016;52:329–42.
- Tzoumaki MV, Moschakis T, Scholten E, Biliaderis CG. In vitro lipid digestion of chitin nanocrystal stabilized o/w emulsions. *Food Funct.* 2013;4:121–9.
- Zhang R, Zhang Z, Zhang H, Decker EA, McClements DJ. Influence of emulsifier type on gastrointestinal fate of oil-in-water emulsions containing anionic dietary fiber (pectin). *Food Hydrocoll.* 2015;45:175–85.
- Zhao Y, Du W, Sun L, Yu L, Jiao J, Wang R. Facile synthesis of calcium carbonate with an absolutely pure crystal form using 1-butyl-3-methylimidazolium dodecyl sulfate as the modifier. *Colloid Polym Sci.* 2013;291:2191–202.
- Ranjan R, Narnaware SD, Patil NV. A novel technique for synthesis of calcium carbonate nanoparticles. *Natl Acad Sci Lett.* 2018;41:403–6.
- Raudsepp P, Brüggemann DA, Lenferink A, Otto C, Andersen ML. Oxidative stabilization of mixed mayonnaises made with linseed oil and saturated medium-chain triglyceride oil. *Food Chem.* 2014;152:378–85.
- Shao Y, Tang C-H. Gel-like pea protein Pickering emulsions at pH3.0 as a potential intestine-targeted and sustained-release delivery system for β -carotene. *Food Res Int.* 2016;79:64–72.

41. Xiao J, Li C, Huang Q. Kafirin nanoparticle-stabilized pickering emulsions as oral delivery vehicles: physicochemical stability and in vitro digestion profile. *J Agric Food Chem*. 2015;63:10263–70.
42. Xiao J, Wang Xa P, Gonzalez AJ, Huang Q. Kafirin nanoparticles-stabilized Pickering emulsions: Microstructure and rheological behavior. *Food Hydrocoll*. 2016;54:30–9.
43. Narukulla R, Ojha U, Sharma T. Enhancing the stability and redispersibility of o/w Pickering emulsion through polyacryloyl hydrazide-tannic acid synergy. *Colloids Surf A Physicochem Eng Asp*. 2019;568:204–15.
44. Kumar N, Gaur T, Mandal A. Characterization of SPN Pickering emulsions for application in enhanced oil recovery. *J Ind Eng Chem*. 2017;54:304–15.
45. Sims RJ. Oxidation of fats in food products. *Inform*. 1994;5(1020):1022–8.
46. McClements DJ, Li Y. Review of in vitro digestion models for rapid screening of emulsion-based systems. *Food Funct*. 2010;1:32–59.

Publisher's note

Springer Nature remains neutral with regard to jurisdictional claims in published maps and institutional affiliations.